Soil & Tillage Research 186 (2019) 300–309

Contents lists available at ScienceDirect

Soil & Tillage Research

journal homepage: www.elsevier.com/locate/still

Wheel load, repeated wheeling, and traction effects on subsoil compaction in northern Europe

Mansonia Pulido-Moncada*, Lars J. Munkholm, Per Schjønning

Aarhus University, Department of Agroecology, Research Centre Foulum, Blichers Allé 20, P.O. Box 50, DK-8830 Tjele, Denmark

ARTICLE INFO

Keywords:
Wheel load
Repeated wheel passes
SubVESS
Soil pore size distribution
Air permeability
Gas diffusivity
Degree of compaction

ABSTRACT

Traffic in agricultural fields with very high wheel loads imposes a risk of severe structural damage deep into the subsoil. However, there is a paucity of studies quantifying these effects. This study focuses on heavy traffic-induced changes in soil structure for a sandy loam soil in a temperate region. The treatments included no compaction (Control), compaction with ~3 Mg (M3) and ~8 Mg (M8) wheel loads with multiple (4–5) wheel passes, and compaction with a single-pass wheel load of ~12 Mg (S12). The compaction treatments were replicated four consecutive years. Subsoil structural quality was evaluated visually by the SubVESS method, and soil pore characteristics were quantified for minimally disturbed soil cores sampled at 30, 50, 70 and 90 cm depth two years after the end of the experiment. Our results indicate that M8 significantly affected soil structural properties to > 50 cm depth in terms of reduced subsoil structural quality, air-filled pore space, air permeability, gas diffusivity, pore volume and increased bulk density. Results also showed that the degree of compactness was ≥95% for M8 at 30 and 50 cm depth. Even though a pre-existing dense soil matrix was described in the studied soil, results confirmed that high wheel loads may cause significant subsoil compaction at > 50 cm depth. Surprisingly, the S12 treatment did not show marked signs of decreasing structural quality at depth. Thus, our results indicate that primarily traffic applying multiple passes with high wheel loads compromises soil structure at depth. The S12 results further suggest the need to investigate the influence of factors other than wheel load and inflation pressure on the risk of subsoil compaction.

1. Introduction

Soil compaction is one of the major problems in agricultural soils across the globe. Field traffic with heavy machinery is the main cause of top and subsoil compaction - affecting 33 million ha of land in Europe (FAO, ITPS, 2015). In temperate regions like North-western Europe, the problem of soil compaction has been worsened by the increasing size of agricultural machinery (e.g. Vermeulen et al., 2013; Schjønning et al., 2015), but also by inappropriate management of soil in unfavourable moisture conditions (Hamza and Anderson, 2005).

Soil compaction due to vehicular traffic in too wet conditions induces soil structure deterioration and soil deformation, which affects soil structure-related properties such as aeration, soil strength and structural characteristics (Lipiec and Hatano, 2003; Zink et al., 2011), which consequently affects crop growth and yield (Håkansson and Reeder, 1994). Subsoil compaction might besides compromise the soil's ability to mitigate effects from agriculture on the environment. For instance, anoxic spots in compacted soil may increase production and emission of greenhouse gases (O'Sullivan and Vinten, 1999), and preferential flow of pollutants in macropores may result from compaction-induced reduction in marginal pores (Schjønning et al., 2013).

The degree of damage associated with soil compaction depends on several factors and their interaction. The early modelling work of Söhne (1958) concluded that wheel load is a significant driver of the stress transmitted to deep soil layers. Further, studies covering a range of different soil types have reported significant compaction effects on structural conditions to deep subsoil layers (e.g., Jakobsen and Greacen, 1985; Voorhees et al., 1986; Alakukku, 1996; Berisso et al., 2012). Despite this documentation, different opinions exist on the possibility of sustainable traffic with heavy machinery. According to Ansorge and Godwin (2007), the use of tracks has the potential to distribute the load on a larger contact area and hence allow for high loads. Hadas (1994) acknowledged the general validity of the Söhne (1958) model but made a plea for taking into account a range of aspects affecting stress transmission in the soil profile. It is though clear from several studies that the wheel load has a dominating effect in deep soil layers (Arvidsson and Keller, 2007; Horn and Fleige, 2009; Lamandé and Schjønning, 2011).

Tyre inflation pressure is known to be a key driver for traffic effects

* Corresponding author.
E-mail addresses: mansonia.pulido@agro.au.dk (M. Pulido-Moncada), lars.munkholm@agro.au.dk (L.J. Munkholm), per.schjonning@agro.au.dk (P. Schjønning).

https://doi.org/10.1016/j.still.2018.11.005
Received 12 April 2018; Received in revised form 30 August 2018; Accepted 6 November 2018

Table 1
Total organic carbon, particle size distribution and the Rosin and Rammler (1933) model parameters (α, β) for the Control and compaction treatments. Minimum and maximum values are given in brackets.

Depth (cm)	Treatment[a]	Total organic carbon	Clay	Silt	Sand	α	β
		g 100 g^{-1}	(< 2 μm)	(2–63 μm)	(63–2000 μm)	(μm)	(-)
30	Control	0.57 (0.30-1.29)	11 (07-14)	26 (24-29)	63 (59-69)	210 (181-249)	0.61 (0.54-0.67)
	M3	0.72 (0.52-1.09)	14 (12-17)	32 (28-42)	54 (46-58)	144 (105-163)	0.54 (0.50-0.59)
	M8	0.40 (0.23-0.47)	10 (04-15)	29 (26-33)	61 (57-70)	172 (157-206)	0.65 (0.52-0.86)
	S12	0.75 (0.57-0.83)	12 (10-16)	27 (24-31)	61 (53-66)	192 (138-245)	0.57 (0.49-0.63)
50	Control	0.13 (0.11-0.16)	12 (07-15)	26 (19-31)	62 (54-69)	200 (153-249)	0.59 (0.53-0.70)
	M3	0.31 (0.15-0.70)	16 (11-20)	29 (24-37)	55 (51-59)	153 (126-180)	0.53 (0.45-0.62)
	M8	0.12 (0.06-0.18)	13 (06-19)	25 (19-32)	62 (49-72)	174 (117-230)	0.65 (0.46-0.82)
	S12	0.25 (0.18-0.34)	17 (14-20)	27 (24-32)	56 (52-62)	163 (133-214)	0.49 (0.45-0.52)
70	Control	0.09 (0.07-0.11)	17 (11-24)	28 (24-33)	55 (43-62)	146 (78-195)	0.52 (0.41-0.61)
	M3	0.13 (0.10-0.21)	16 (14-18)	26 (24-28)	58 (56-61)	165 (152-183)	0.51 (0.47-0.54)
	M8	0.09 (0.08-0.09)	18 (15-19)	32 (23-46)	50 (35-62)	129 (57-204)	0.53 (0.48-0.62)
	S12	0.16 (0.10-0.30)	16 (12-20)	25 (21-29)	59 (51-67)	188 (124-289)	0.51 (0.44-0.57)
90	Control	0.07 (0.05-0.10)	20 (13-31)	24 (21-26)	56 (44-65)	156 (79-207)	0.48 (0.34-0.57)
	M3	0.09 (0.06-0.13)	18 (15-22)	29 (23-38)	53 (40-60)	137 (69-175)	0.47 (0.40-0.54)
	M8	0.08 (0.07-0.09)	18 (14-25)	35 (23-61)	47 (21-62)	128 (33-207)	0.51 (0.39-0.57)
	S12	0.11 (0.07-0.20)	16 (15-18)	25 (24-27)	59 (57-62)	185 (167-223)	0.51(0.48-0.52)

[a] Treatment labels indicate the number of wheel passes (M = multiple passes, S = single pass) and the approximate maximum wheel load in Mg.

on the topsoil (e.g., Campbell et al., 1986; Zink et al., 2010). Arvidsson and Keller (2007) indicated the problem in differentiating the inflation pressure from wheel load as the rated pressure increases with wheel load. Schjønning et al. (2012) documented clearly that the stress distribution in the tyre-soil contact area is far from uniform. They showed that the maximum stress in the contact area is close to the mean ground pressure for large, low-pressure tyres, while it may be more than double that for narrow, high-pressure tyres. In that study, Söhne-model predictions with the measured stress distributions as input allowed for an estimate of the relative effect of wheel load and inflation pressure. It appeared that the model-predicted depth of the 50 kPa vertical stress increased ~ 8 cm with each additional Mg wheel load and with ~8 cm for each doubling of the inflation pressure. The prediction equation was validated against measured soil stresses and hence provides an approximation of the relative contribution from load and inflation pressure (Schjønning et al., 2012).

A range of studies has quantified the effect of repeated short-term stress application (e.g. passage of several wheels after each other). Lipiec et al. (1992) found that the vertical deformation of the plough layer soil was linearly related to the logarithm of the number of wheel passes. Even for light-weight traffic, crop yield has been shown to decrease for each additional wheel pass, which emphasizes the paramount influence of topsoil properties on plant growth (Campbell et al., 1986). Two studies on upper subsoil compaction found cone penetration resistance to increase linearly with the number of successive wheelings (Botta et al., 2009; Naderi-Boldaji et al., 2018). Zink et al. (2011) documented a significantly stronger decrease in the subsoil (40 and 60 cm) air-filled pore space after ten compared to a single wheel pass. Horn et al. (2003) outlined the complicated processes in play for soil exposed to repeated wheeling. Different trends in stresses experienced with repeated passes have been observed as indicated by Riggert et al. (2016).

Only a few studies have addressed the effect of shear stresses. Berisso et al. (2013) quantified the mean normal stress and the horizontal stress during the passage of an 80 cm wide implement tyre. Their results indicated shear strain at the periphery of the tyre, which was in line with measured shear stress. The study also found that deviatoric stresses may affect soil pore continuity, which in turn has significant effects on gas transport. Pytka et al. (2006) found that traction affects shear stresses in the upper soil layers whereas soil deformation was very different in passive passes of wheels compared to tractive passes.

Many compaction experiments apply several repeated passes of machinery in the year of establishing the experiment (e.g., Håkansson and Reeder, 1994; Arvidsson, 2001). This has been considered unrealistic for practical farming conditions because changes in stress-strain relations in the soil between traffic events as a consequence of wetting/drying cycles, frost, and biological activity, among others is not taken account of (Koch et al., 2005). Some experiments have investigated the effect of selected field operations expected to be critical for soil properties and crop yields (e.g., Schäfer-Landefeld et al., 2004). Other studies have focused on isolated aspects hypothesised to affect compaction (e.g., Arvidsson and Keller, 2007).

In the present study, we conducted a farm-realistic traffic experiment with equipment commonly used for slurry application. The experimental traffic took place at moist soil conditions on a glacial till soil in a temperate region. The investigation included a range of wheel loads (~ 39–118 kN), tyre sizes (~ 0.30-0.96 m^2 tyre-soil contact area), tyre inflation pressures (150–300 kPa), and a number (1–5) of repeated wheel passes in one traffic event. The effect of four consecutive years of traffic on subsoil structural characteristics was investigated at four soil depths, 30–90 cm. It was hypothesised that the use of modern heavy machinery (wheel loads > 8 Mg) under wet conditions would cause structural damage several decimetres into the subsoil and that the damage on subsoil structure (especially at depth) would increase with wheel load and number of passes.

2. Materials and methods

2.1. Study site description

The study was conducted in an experimental field located at Research Centre Aarslev, Denmark (55° 18′ 18″ N, 10° 26′ 52″E). This site is located at an elevation of 51 m.a.s.l. The Aarslev soil is derived from glacial tills of the Weichselian glaciation and has been classified as Orthic Luvisols in the FAO classification system. The experimental field at Aarslev is a sandy loam soil (Table 1). The mean annual rainfall and temperature for the experimental period (2010–2013) at Aarslev were close to the long-term baseline for 1961–1990 (see Supplementary material Table A in Schjønning et al. (2016)). For 2010–2013, the mean rainfall was 303 mm for October-March and 249 mm for April-July, and the mean temperature was 2.8 and 12.3 °C, respectively. The experimental area is described in detail by Schjønning et al. (2011).

Table 2
Main characteristics of the experimental treatments. The exact wheel loads and inflation pressures for all wheels and all experimental years can be found as 'supplementary materials' in Schjønning et al. (2016). The experimental traffic was applied wheel-by-wheel across the experimental plots.

Treatment[a]	Machinery used	Wheel passes in a traffic event	Approximate max. wheel load[b] (Mg)	Range in inflation pressure (kPa)
M3	A tractor-trailer combination for slurry application	5	3 (2.4–4.0)	150–300
M8		4	8 (1.3–10.1)	150–300
S12	A self-propelled, tricycle-like machine for slurry application	1	12 (7.6–12.1)	150–250

[a] Treatment labels indicate the number of wheel passes (M = multiple passes, S = single pass) and the approximate maximum wheel load in Mg.
[b] Minimum and maximum values are given between brackets.

2.2. Experimental treatments

The experimental treatments are described in detail by Schjønning et al. (2016). Briefly, a four-year compaction experiment was conducted from 2010 to 2013 in a field that was mechanically subsoiled to 40 cm depth approximately six years prior to the start of the experiment. The experimental treatments consisted of annual traffic applied wheel-by-wheel across the plots using different machinery (Table 2). The treatments included no compaction (Control), compaction with ~3 Mg (M3) and ~8 Mg (M8) wheel loads with multiple passes (4–5) by a tractor-trailer combination for slurry application, and compaction with a single-pass wheel load of ~12 Mg (S12) by a self-propelled tricycle-like machine for slurry application. Commonly used tractor-trailer machinery for slurry application in Denmark applies ~ 6 Mg on trailer wheels and with inflation pressures higher than rated for field traffic. The latter reflects the need to allow for high-speed traffic on roads when driving to and from the fields. In this study, we simulated reduced-load traffic by emptying the slurry trailer (M3) and high-load traffic by driving with a full trailer with the front axle hydraulically lifted (M8). The self-propelled machinery used for the S12 treatment allowed for on-the-go regulation of inflation pressures. Hence, the inflation pressures for this treatment reflect the manufacturer's recommendation for traffic in the field.

The experimental treatments were replicated four times in a randomised block design with plots measuring 10 × 30 m. The compaction treatments were applied in spring at a soil water content near field capacity. Spring barley (*Hordeum vulgare* L.) was annually established after a shallow secondary tillage (~ 5 cm depth) in all experimental plots. The present study reports results for soil samples taken two years after completion of the four-year compaction experiment. The treatments are denoted M3, M8 and S12 in the following. Treatment labels indicate the number of wheel passes (M = multiple passes, S = single pass) and the approximate maximum wheel load in Mg.

2.3. Field measurements

The visual evaluation of subsoil structure (SubVESS) method of Ball et al. (2015) was applied on 16 soil profiles (four treatments x four blocks). The upper and lower depth limits of assessment were below 20 cm and to approximately 1 m, respectively. For each soil profile, layers of contrasting colour and hardness were identified. The SubVESS method requires individual evaluation of each soil layer by observing and scoring the following indicators as key diagnostic factors: mottling (degree of anaerobism), strength (resistance of the soil to penetration by a knife), porosity (presence of visible pores and voids), pattern and depth of root penetration, and aggregate size/shape. Scoring of the indicators is based on a scale of 1–5, where 1 is best and 5 is worst. The overall score of the subsoil structural quality (Ssq) is based on the score of the five indicators and the SubVESS description given in the flowchart (Ball et al., 2015).

2.4. Laboratory measurements and analyses

In the same pits as used for SubVESS, three sampling spots were randomly selected, where undisturbed 100-cm^3 soil cores were taken vertically at 30, 50, 70 and 90 cm depth. For each treatment, a total of 144 cores were sampled (four depths × four blocks × three sampling spots × three replicate cores). Soil cores were kept at 2 °C until laboratory measurements and analyses were conducted. The soil cores were saturated by capillarity and then drained at −10, −50, −100 and −300 hPa matric potentials to obtain water release data. Water content at −1.5 MPa was estimated from the pedotransfer function developed by Hansen (1976) for Danish soils:

$$w_{1.5\,MPa} = (0.38 \times clay) + (0.76 \times SOM) \quad (1)$$

where $w_{1.5MPa}$ is the gravimetric water content at −1.5 MPa (g g^{-1}), *clay* is the clay content and *SOM* is the soil organic matter content, both in g 100 g^{-1} soil minerals.

Pore size frequency curves were derived from the water release curve by numerical differentiation (Schjønning, 1992). This approach enables a more comprehensive analysis of the water release data and allows distinction between a unimodal and bimodal pore size distribution. Briefly, a spline interpolation procedure was used to yield discrete interpolated values on the sum curve relating pore diameter to accumulated pore volume. The sum curve was extrapolated to high pF values, setting the water content to zero at pF = 7.0 and total pore volume at pF = 0. The frequency curve was produced by a numerical differentiation procedure.

At −100 hPa matric potential, air permeability (k_a), air-filled porosity (ε_a) and gas diffusivity were measured sequentially. k_a was quantified using the Forchheimer approach (1901) with an apparatus that allows automatic measurement of air flow at a range of pneumatic pressures (Schjønning and Koppelgaard, 2017). In the apparatus, a core sample is enclosed in the measuring chamber by an inflatable rubber O-ring to prevent air leakage. A measurement loop basically includes measurements of the four corresponding values of the pressure difference, ΔP, and air flow, Q. The true Darcian air permeability is calculated based on a polynomial regression of flow-pressure data (Schjønning and Koppelgaard, 2017).

An air pycnometer was used to measure the fraction of soil air-filled porosity connected to the atmosphere (ε_a) (Rüegg, 2000; Flint and Flint, 2002). Briefly, soil samples were placed in a closed chamber with automatic measurements of corresponding values of volume at two pressures. The ε_a of each soil sample was derived from calculations based on Boyle's law.

Gas diffusivity was measured using the one-chamber, one-gas method described by Schjønning et al. (2013). Fick's second law applies to this non-steady state diffusion and hence allows the calculation of the gas diffusion coefficient in soil (D_s). The relative diffusivity (D_s/D_o) was calculated by relating D_s to the diffusion of O_2 in the air, D_o (0.205 cm^2 s^{-1} at 20 °C and atmospheric pressure; Smithsonian Physical Tables).

The specific permeability, *SP*, based on the relationship between k_a and ε_a, ($SP = k_a/\varepsilon_a$) (Groenevelt et al., 1984) was used to determine whether differences in k_a are simply related to differences in ε_a, or whether other air-filled pore geometrical parameters such as pore size distribution, tortuosity and continuity are involved.

The pore characteristics indices derived from the tube model proposed by Ball (1981) were also calculated. These are the tortuosity (τ),

the effective pore diameter (d_{eff}), and the number of soil pores per unit transect (n_B), using Eqs. (2)–(4), respectively.

$$Tortuosity = \sqrt{\frac{\varepsilon_a}{D_s/D_o}} \quad (2)$$

$$Effective\ pore\ diameter = \sqrt{\frac{8k_a}{D_s/D_o}} \quad (3)$$

$$Number\ of\ pores = \frac{\varepsilon_a^{1/2}\left(D_s/D_o\right)^{3/2}}{8\pi K_a} \quad (4)$$

where ε_a is soil air-filled pore space connected to the atmosphere, D_s/D_o is the relative gas diffusivity, and k_a is air permeability.

Soil cores were then oven-dried at 105 °C in order to calculate soil dry bulk density (D_b) from the dry mass of each soil core. Total pore volume (TPV) was calculated from the measured D_b and the particle density (D_p), with the latter estimated by a pedotransfer function developed by Schjønning et al. (2017b):

$$D_p = 2.652 + (0.216 \times clay) - (2.237 \times SOM) \quad (5)$$

where D_p is in Mg m^{-3}, and *clay* and *SOM* are in units of kg kg^{-1} soil minerals.

Finally, the degree of compactness, *DC*, was calculated from the measured D_b divided by the reference bulk density (D_{ref}). The D_{ref} was calculated by Eq. (6) using the Rosin–Rammler parameters α and β (Rosin and Rammler, 1933) (Table 1), and SOM content (Keller and Håkansson, 2010):

$$D_{ref} = 1.508 + 0.226\log\alpha - 0.417\,\beta + 0.110\,\beta^2 - 0.0242\,SOM - 0.0110\,SOM\log\alpha \quad (6)$$

2.5. Statistical analyses

Nonparametric Kruskal-Wallis rank sum tests were conducted to detect statistical differences between treatments for SubVESS indicators. A mixed model with compaction treatment as a fixed effect and block as well as treatment × block interaction as random effects was used to evaluate compaction effects on pore characteristics and bulk density. The sampling spot effect nested within the experimental plot (treatment × block) was also treated as a random effect in the model. To ensure the efficiency of the model, principal assumptions were checked and $\log_{10}$ transformation was applied to k_a, *SP*, $_{deff}$ and n_B data. All tests were conducted at the 5% significance level. The analyses were performed using the statistical package SPSS (version 24, SPSS Inc., USA).

3. Results

3.1. Visual structure evaluation

In general, three contrasting layers were distinguished on each of the soil profile pits. For each identified layer separate evaluation of subsoil structural quality was conducted (Table 3). For all treatments, none or diffuse mottling was observed at ~ 25 to ~ 50 cm (layer 1), but well-defined rust-coloured spots were observed at ~ 50 to ~70 cm (layer 2) and ~ 70 to ~ 90 cm depth (layer 3). Mottling was not significantly affected by treatments ($P > 0.05$) in any of the subsoil layers. The soil strength was assessed as moderate (score "3" for Control, M3 and S12) to high (score "4" for M8) in layer 1 with no significant difference between the treatments ($P > 0.05$). In layer 2, a significantly higher soil strength was found for M8 (3.5) compared to Control (2.0) ($P < 0.05$). Low to moderate strengths (score 2.0–3.0) were observed in layer 3 for all treatments (no significant difference). Significantly less visually assessed porosity was present in M8 compared to Control ($P < 0.05$) for layer 1. For layers 2 and 3, none or few pores were observed among the treatments ($P > 0.05$). Roots were mainly observed growing in cracks along the soil profiles. Distinction in treatments was only observed for layer 1, where roots were more restricted in M8 compared to Control ($P < 0.05$). The M8 treatment affected the aggregate size/shape compared to Control in layer 1 ($P < 0.05$). No differences among treatments were observed in layer 2 for this indicator, but M8 and S12 affected differently the aggregates in layer 3. The overall score for subsoil quality showed that the M8 treatment scored significantly higher than Control in layers 1 and 2 and S12 in layer 3 ($P < 0.05$). The M8 scored Ssq 4.0, 3.8 and 3.5, respectively, for layer 1, 2 and 3, which means that it ranged from "compact" (Ssq 4) to an intermediate state between "some compaction" (Ssq 3) and "compact" (Ssq 4).

3.2. Pore size distribution

The results obtained indicate that the pore size frequency curves for the Aarslev soil exhibits two peaks for all depths (Fig. 1). At 30 and 50 cm depth, compaction treatments caused a decrease in the volume of pores > 10 µm, and a corresponding increase in the volume of pores < 10 µm (Fig. 1).

At 30 cm depth, the peaks of the curves showed the negative effect of compaction treatments on pores < 10 µm (M3 > M8 ≥ S12), and this was confirmed by the pore fractions derived from a mass balance (Table A, Supplementary material) ($P < 0.05$). However, the pore fractions showed that only M8 reduced the proportion of pores 60–300 µm ($P < 0.05$) compared to Control at 30 cm depth. In the case of pores of 30–60 µm, M3 had the lowest volume among the treatments ($P < 0.05$).

At 50 cm depth, the peak of small pores (~1 µm) was highest for M8, followed in decreasing order by M3, S12 and Control. Pore size distribution curves also showed a clear reduction of the volume of large pores (> 10 µm) induced by the compaction treatments at 50 cm depth. This corresponds with a significantly lower proportion of pore fractions with diameter > 300, > 60, > 30 and > 10 µm for M8, and with a significant reduction in the proportion of pores 60–300 µm ($P < 0.05$) for all compaction treatments compared to Control at this depth (50 cm).

There were no major differences in pore size frequency among treatments at 70 and 90 cm depth. However, the pore size frequency curves showed that the volume of pores > 100 and > 300 µm was larger for M3 and S12 than for Control at both 70 and 90 cm depth. This is consistent with the significantly larger volume of large pores ($P > 0.05$) for M3 than for Control at 70 cm (> 300 µm) and at 90 cm depth (> 30, > 60 and > 300 µm).

For TPV and D_b there was only a significant difference between treatments at 50 cm depth, where TPV was smallest and D_b largest for M8 and the largest (TPV) / smallest (D_b) for M3 while Control had intermediate values ($P < 0.05$) (Table A, Supplementary material). However, M8 tended to have a higher D_b than Control at 30 cm depth ($P = 0.08$).

3.3. Pore characterisation

The k_a results show significantly lower values for M8 than Control ($P < 0.05$) for 30 and 50 cm depths (Table 4). No significant differences were found among treatments at 70 cm depth ($P > 0.05$). At 90 cm depth, higher values of k_a ($P < 0.05$) were found for M3 and S12 compared to Control.

Air-filled pore volume (ε_a) in contact with the surrounding atmosphere at −100 hPa potential did not differ significantly among treatments at $P = 0.05$ (Table 4) at 30, 70 and 90 cm depth. The ε_a for M3 ($P = 0.07$) and M8 ($P = 0.07$) soil tended to be significantly lower compared to the Control at 30 cm depth. At 50 cm depth, the M8 and S12 treatments had lower values of ε_a ($P < 0.05$) compared to Control.

Table 3
Median of subsoil structural quality scores from a temperate sandy loam soil two years after completion of compaction experiment with different traffic stresses.

Layer	Treatment[a]	Layer upper boundary (cm)	Layer lower boundary (cm)	Mottling	Strength	Porosity	Roots	Aggregates size/shape	Ssq
1	Control	25 (1.7)	48 (4.7)	3.3 (1.3) A	3.0 (0.0) A	3.0 (0.0) A	3.0 (0.2) A	3.0 (0.2) A	3.0 (0.0) A
	M3	26 (1.3)	49 (1)	2.0 (1.1) A	3.0 (0.4) A	3.0 (0.2) AB	3.0 (0.0) AB	3.4 (0.4) AB	3.0 (0.2) AB
	M8	26 (2.7)	51 (4.1)	2.0 (1.1) A	4.0 (0.6) A	4.0 (0.5) B	3.8 (0.4) B	4.1 (0.2) B	4.0 (0.0) B
	S12	25 (0.0)	49 (6.5)	2.0 (0.0) A	3.0 (0.2) A	3.5 (0.4) AB	3.0 (0) AB	3.3 (0.4) AB	3.0 (0.4) AB
2	Control	48 (4.7)	75 (10.5)	4.5 (0.0) A	2.0 (0.2) A	5.0 (0.9) A	2.8 (0.4) A	2.5 (0.4) A	2.5 (0.2) A
	M3	49 (1.0)	77 (7.4)	4.5 (1.1) A	2.3 (0.4) AB	3.8 (0.7) A	2.8 (0.4) A	2.8 (0.3) A	2.8 (0.4) AB
	M8	51 (4.1)	82 (2.1)	4.5 (0.0) A	3.5 (0.6) B	5.0 (0.9) A	3.0 (0.4) A	3.8 (0.5) A	3.8 (0.3) B
	S12	49 (6.5)	79 (6.1)	4.5 (0.0) A	2.3 (0.4) AB	5.0 (0.9) A	3.0 (0.2) A	2.8 (0.4) A	2.8 (0.3) AB
3	Control	75 (10.5)	98 (4.3)	4.5 (0.0) A	2.5 (0.5) A	5.0 (0.0) A	2.5 (0.5) A	2.3 (0.4) AB	2.8 (0.4) AB
	M3	74 (6.3)	100 (0.0)	4.5 (0.0) A	2.0 (0.5) A	5.0 (0.0) A	3.0 (0.5) A	2.0 (0.2) AB	2.5 (0.2) AB
	M8	82 (2.1)	100 (0.0)	4.5 (0.0) A	3.0 (0.4) A	5.0 (0.0) A	3.0 (0.0) A	3.0 (0.0) B	3.5 (0.0) B
	S12	79 (6.1)	100 (0.0)	4.5 (0.0) A	2.0 (0) A	5.0 (0.0) A	2.5 (0.5) A	2.0 (0.2) A	2.5 (0.0) A

Ssq = subsoil structural quality score; lower values refer to better soil quality (Ball et al., 2015). Standard deviation is given in parenthesis (±). Values in a column followed by the same letter are not significantly different among treatments in the same layer (Kruskal-Wallis' test, P = 0.05).

[a] Treatment labels indicate the number of wheel passes (M = multiple passes, S = single pass) and the approximate maximum wheel load in Mg.

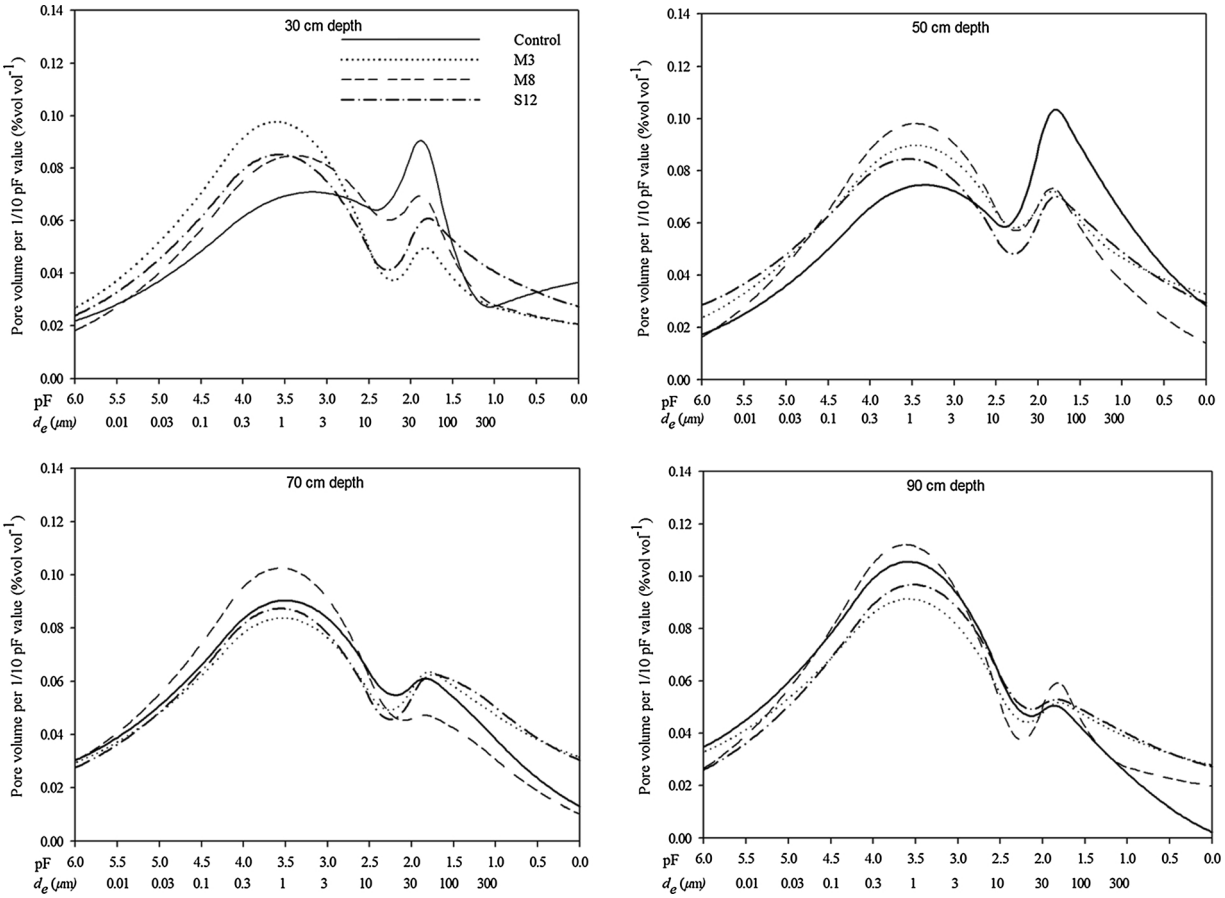

Fig. 1. Pore size distribution as a function of matric potential at 30, 50, 70 and 90 cm depth in Control and compaction treatments. Pore size distribution was obtained by numerical differentiation (Schjønning, 1992). Compaction treatment labels indicate the number of wheel passes (M = multiple passes, S = single pass) and the approximate maximum wheel load in Mg. Pore volumes in specific pore size classes are given in the supplementary material.

At 30 cm depth, D_s/D_o was significantly smaller only for M3 ($P < 0.05$) compared to Control (Table 4), although D_s/D_o for M8 tended to also be lower compared to Control ($P = 0.08$). At 50 cm depth, only the M8 treatment differed from Control for D_s/D_o ($P < 0.05$) (M8 < Control). D_s/D_o did not differ significantly among treatments at 70 and 90 cm depths.

The smallest value of specific permeability (*SP*) was found for the M3 ($P = 0.059$) and M8 ($P = 0.055$) treatments compared to Control at 30 and 50 cm depths, respectively. No significant differences were found at 70 cm depth, but larger values of *SP* were obtained for M3 and S12 compared to Control ($P < 0.05$) at 90 cm depth.

In the soil profile, tortuosity (τ) ranged from 3.4 to 4.9. At 30 cm depth, the soil under M3 and M8 exhibited significantly greater τ than Control ($P < 0.05$), but at 50 cm depth this was only the case for M8. Compaction treatments did not significantly affect τ at 70 cm depth, but at 90 cm depth τ was lower for M3 and S12 compared to Control ($P < 0.05$).

At 30 cm depth, the d_{eff} was significantly smaller for M8 (66 μm) than for M3 (110 μm) and S12 (104 μm) while the Control displayed an intermediate value (85 μm). The significantly smallest n_B was estimated for M3 (36 per cm^2) as compared to 125 per cm^2 for Control at 30 cm depth. At 50 cm depth, the M3 treatment had larger d_{eff} and smaller n_B

Table 4
Soil pore characteristics at −100 hPa matric potential. Air permeability (k_a), specific permeability (*SP*), effective pore diameter (d_B) and number of soil pores (n_B) are given as geometric means.

Depth (cm)	Treatment[a]	k_a (μm^2)	ε_a (m^3 m^{-3})	D_s/D_o ×1000	*SP*	Tortuosity	d_{eff} (μm)	n_B (−cm^2)
30	Control	7.1 B	0.136 A	9.1 B	61 AB	4.1 A	85 AB	125 B
	M3	5.7 AB	0.083 A	4.1 A	74 B	4.9 B	110 B	36 A
	M8	2.3 A	0.080 A	4.7 AB	30 A	4.8 B	66 A	63 AB
	S12	9.0 B	0.109 A	7.8 AB	93 B	4.2 AB	104 B	58 AB
50	Control	13.8 B	0.166 C	14.3 B	95 AB	3.4 A	88 AB	150 B
	M3	25.5 B	0.141 BC	12.0 AB	187 B	3.6 AB	146 C	56 A
	M8	5.7 A	0.101 A	8.7 A	67 A	3.8 B	95 B	52 AB
	S12	16.9 B	0.131 AB	12.1 AB	123 AB	3.6 AB	116 BC	83 AB
70	Control	7.7 A	0.098 A	6.9 A	87 A	4.0 A	100 A	64 A
	M3	19.9 A	0.129 A	8.7 A	157 A	3.9 A	130 B	53 A
	M8	7.2 A	0.093 A	6.7 A	86 A	4.3 A	109 AB	53 A
	S12	14.4 A	0.133 A	9.4 A	118 A	3.9 A	116 AB	74 A
90	Control	4.4 A	0.079 A	4.5 A	62 A	4.8 B	104 A	33 A
	M3	14.6 BC	0.107 A	6.7 A	141 B	4.3 A	132 B	34 A
	M8	7.6 AB	0.086 A	4.8 A	97 AB	4.5 AB	125 B	33 A
	S12	15.1 C	0.110 A	8.3 A	145 B	4.0 A	134 B	39 A

ε_a = air-filled pore space in contact to the atmosphere when drained to a matric potential of −100 hPa (excluding blocked pore volume). D_s/D_o = relative diffusivity, where D_s and D_o are the diffusion coefficients in soil and in air, respectively. $SP = k_a/\varepsilon_a$. Tortuosity = $[\varepsilon_a/(D_s/D_o)]^{0.5}$. $d_{eff} = [(8k_a)/D_s/D_o]^{0.5}$. $n_B = [(\varepsilon_a{}^{1/2})(D_s/D_o)^{3/2}]/(8\pi k_a)$. Values in a column followed by the same uppercase letter are not significantly different among treatments in the same depth (P = 0.05).

[a] Treatment labels indicate the number of wheel passes (M = multiple passes, S = single pass) and the approximate maximum wheel load in Mg.

values compared to the Control treatment (P < 0.05). At 70 cm depth, M3 had larger d_{eff} values than Control, but there were no significant differences in n_B. At 90 cm depth, the experimental plots with compaction treatments had larger d_{eff} values than the Control soil, whereas no differences were found for the n_B (P < 0.05).

3.4. Reference bulk density and degree of compactness

The calculated D_{ref} varied from 1.74 to 1.83 Mg m^{-3} depending on clay and organic matter content (Eq. (6)) (data not shown). The *DC* varied from 88 to 101% for the different treatments, with the highest value estimated for M8 at 30 cm depth (Fig. 2). At 30 and 50 cm depth, the *DC* was significantly higher for M8 compared to Control (P < 0.05) and at 70 cm *DC* was significantly higher for M8 than for S12. No differences among treatments were found for *DC* at 90 cm depth.

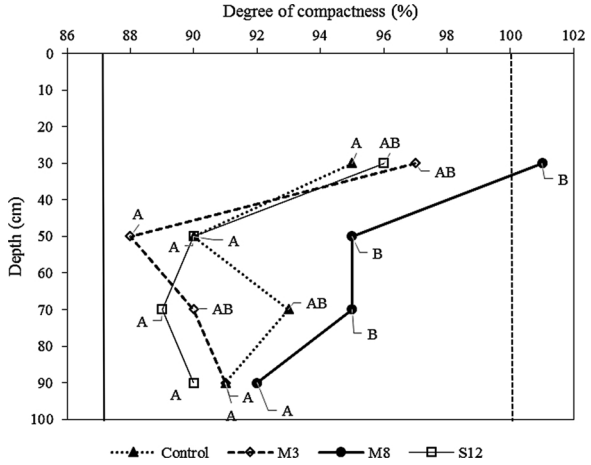

Fig. 2. Degree of compactness (*DC*) for Control and compaction treatments in the subsoil. Treatment labels indicate the number of wheel passes (M = multiple passes, S = single pass) and the approximate maximum wheel load in Mg. *DC* was calculated from the measured bulk densities divided by the reference bulk densities. Reference bulk densities were estimated using the Eq. (13) of Keller and Håkansson (2010), where the Rosin–Rammler parameters α and β, and soil organic matter content are the estimated factors. Values followed by the same uppercase letter are not significantly different among treatments in the same depth (P = 0.05). Solid line at 87% of *DC* is the critical limit for spring barley topsoil (Håkansson and Lipiec, 2000).

4. Discussion

4.1. Visual soil structural quality evaluation

The mottling and poorly visible porosity observed for Control from ~ 50 to ~ 90 cm depth evidence a preceding limited aeration for the studied subsoil. The poor structural quality (hard and dense structural units and poor drainage) described for the M8 treatment in the upper subsoil (~ 25-50 cm) confirm the results of Schjønning et al. (2017a). Please note that all treatments received a score of 3 or higher for layer 1, showing that at least "some compaction" was present in all cases, despite the soil being mechanically loosened to a depth of ~ 40 cm six years prior to the start of the compaction experiment.

The SubVESS evaluations indicate the existence of a negative effect of the mechanical stresses caused by M8 up to ~75 cm depth. Surprisingly, the highest wheel load treatment, S12, did not show visual signs of increased compaction (compared to Control) at any depth. Thus, the subsoil structural quality assessment surprisingly suggests that a high wheel load with a single wheel pass does not induce apparent morpho-structural changes (discussed in further detail below). Results from the visual soil evaluation, showing the negative effect of soil compaction by a heavy tractor with ~8 Mg wheel load on soil morphological characteristics, are consistent with previous studies conducted in a sandy soil classified as Glossic Phaeozem (e.g., Obour et al., 2016).

4.2. Compaction effects on soil pores

From a visual judgment, the two peaks shown in the pore size frequency curves indicate that the investigated soil has a bi-modal pore size distribution (Fig. 1). The pores making up the volume around these two peaks have been labelled the textural and the structural pores, respectively (Dexter et al., 2008). Textural pores involve small matrix and residual pores within aggregates, whereas structural pores are large pores (Dexter et al., 2008). At both 30 and 50 cm depth, the Control soil showed a high peak for structural porosity (~ 50–70 μm), which fairly dominated the shape of the curve. At 30 and 50 cm depth, structural deformation by compaction treatments reduced the volume of structural pores, becoming smaller than the textural. Pore fractions shown in

Table A, Supplementary material, support the clear differences among the M8 pore size distribution curve relative to the Control at 50 cm depth. Note that textural pores (peak at ~ 1 μm) were more dominant at 70 and 90 cm than at 30 and 50 cm depth (especially for the Control treatment). We consider that the observations for 70 and 90 cm depths are much affected by the pronounced textural variation across the experimental field (Table 1).

Our results are in accordance with measurements on another glacial till soil (Berisso et al., 2012). Applying the double-exponential model for pore size distribution (Dexter et al., 2008), Berisso et al. (2012) found a significantly lower volume of structural pores reflecting the large-diameter peaks in Fig. 1. Although in the present study, the differences between compaction treatments and Control were not always significant for pore characterisation parameters in the 30 and 50-cm soil layers, the mainly bi-modal pore size distribution for the compaction treatments is clear evidence of the reorganization of the soil particles in the soil and the impact of the mechanical stress on the soil. The pore fractions estimated (Table A, Supplementary material) did suggest that the changes in pore size induced by compaction treatments are mainly reflected in the pore size ranges 60–300, 10–300 and 30–60 μm. Eden et al. (2011) also obtained pore size curves showing a decreased volume of pores > 10 μm after soil compaction on a loamy sand soil, which correlated with a reduction in the soil's ability to conduct gases.

The generally higher k_a values (Table 4, 30 cm depth) compared to those found after three years of compaction (Schjønning et al., 2017a) relate to the improved Forchheimer methodology (Schjønning and Koppelgaard, 2017) for estimating Darcian flow used in this study. However, notably the trend between treatments is the same as after three years of experimentation. I.e., Control, M3 and S12 were approximately identical with M8 showing significantly lower permeability. Hence, M8 significantly reduced k_a compared to Control, by 67 and 59%, at 30 and 50 cm depth, respectively (Table 4). Permeability classification by Fish and Koppi (1994) indicates limited or low air permeability when $k_a \leq 20\,\mu m^2$. Our results show k_a values ranging from 4.4 to 13.8 μm^2 for Control in the soil profile, which indicates restricted conditions generally for air flow for the experimental field. Importantly, the k_a for M8 at 30 cm depth (2.3 μm^2) was close to the limit for impermeable soil of 1 μm^2 according to Ball et al. (1988). This indicates that biological processes for M8 at 30 cm depth are potentially restricted due to limited water and air transport (Ball et al., 1988). Additionally, low values (< 10 μm^2) were also observed for M3 and S12 at 30 cm depth, and for M8 at 50, 70 and 90 cm depth. However, values of k_a at 90 cm depth are probably related to textural variation (Table 1).

The M3 and M8 treatments exhibited lower ε_a values at −100 hPa (corresponding to field capacity) than the critical ε_a limit (0.1 $m^3\,m^{-3}$) for plant growth (Grable and Siemer, 1968) at 30 cm depth. Importantly, most values were close to the 0.1 $m^3\,m^{-3}$ limit. This, together with the k_a results, confirms the poor porosity visually observable in the subsoil for all treatments and depths.

In the Groenevelt et al. (1984) study the magnitude of k_a was found to be influenced by the magnitude of ε_a, and they proposed the ratio $SP = k_a/\varepsilon_a$ to provide a more neutral interpretation consisting simply of the permeability normalized to a unit volume of air-filled pores space (Schjønning et al., 2013). A reduction in *SP* was found for M8 compared to Control at 30 and 50 cm depth. This indicates that other aspects than just the air-filled pore volume have influenced the convective air transport and concords with the increase in τ for this treatment (Table 4). A small *SP* value reflects a dense and homogeneous matrix (Schjønning and Thomsen, 2013).

The S12 treatment caused neither changes in the above-described parameters nor in D_s/D_o. In contrast, M3 reduced D_s/D_o by 55% at 30 cm depth, and M8 reduced D_s/D_o by 48% and 39% at 30 and 50 cm depth, respectively, when compared with Control. Critical conditions for aerobic life processes have been estimated to prevail when D_s/D_o becomes lower than a threshold that ranges from 0.005 to 0.02 (Stepniewski, 1980, 1981). This was confirmed by Schjønning et al. (2003), who found the lower range threshold (D_s/D_o = 0.005) to be valid for two soils containing 0.22 and 0.34 kg kg^{-1} clay, respectively. For a soil with a clay content of ~ 0.11 kg kg^{-1}, the critical threshold was closer to the D_s/D_o = 0.02 value. Based on this, our results reveal low gas diffusivity in the subsoil for both the Control and compaction treatments (Table 4). Especially small values of D_s/D_o were measured for M3, M8 and S12 at 30 cm depth, as well as for M8 at 50 cm depth (D_s/D_o range from 0.004-0.014). Our results chime with those of Berisso et al. (2012), who found high-wheel load field traffic reduced D_s/D_o at 30, 50, 70 and 90 cm depths of a glacial till soil, but only significantly so for the 30 cm depth.

Interestingly, the two tractor-trailer systems, M3 and M8, displayed significantly higher soil pore tortuosities than the Control, which had a value close to that for S12 (Table 4). Similarly, the dense and homogeneous matrix described for soil under M8 appears to be more tortuous than Control down to 50 cm depth. This may be related to high horizontal traction stresses for the tractor-trailer system as discussed further below. For the two upper soil layers (30 and 50 cm), we note that all three compaction treatments tended to reduce the n_B in a cross-sectional area of the soil (Table 4). The effect was significant for the M3 treatment. This may be interpreted as an effect of the mechanical stresses on the small, marginal pores in between vertical biopores (Schjønning et al., 2013). Now, given approximately identical (high) tortuosities and (low) n_B for the two tractor-trailer systems (M3 and M8), it is noticeable that M8 for both 30 and 50 cm depth is estimated to have smaller d_{eff} than M3 (Table 4).

Differences between M3 and M8 in terms of d_{eff} most likely indicate a compaction-induced reduction in the diameter of the dominating, vertical (bio)pores active in the convective flow (Schjønning et al., 2013). This is supported by the *SP* indicator, which is significantly lower for M8 than for M3; the anticipated reduced diameter of the vertical biopores will reduce the convective flow according to Poiseuille's law. However, for the upper two soil layers, we note a trend of increasing effective diameter of the M3 compared to Control (significantly for the 50 cm depth; Table 4). This in turn probably reflects the smaller number of pores for compacted soil; compaction tends to turn the soil from a sponge-like matrix to a solid with some hollow tubes. The quantification of the tube model for pore characteristics suggests that the compaction treatments close the marginal pores leaving the vertical biopores open for more direct flow, although with a narrower diameter with increasing mechanical stress. The findings agree well with the comprehensive study conducted by Schäffer et al. (2008), which indicates that the diameter of the large cylindrical pores and the interaggregate pores decreased with increasing compression. The study also notes that large vertical pores are less sensitive to compaction than smaller interaggregate pores, irrespective of their initial diameter and orientation. This caused an increase in the average pore diameter until the cylindrical pores were severely affected by high compression load.

Changes in the geometry of the pore system have been reported as a persistent consequence of soil compaction (Etana et al., 2013). Interestingly, none of the above trends in soil pore characteristics were significantly different between the Control soil and the S12 treatment. Notably, in our study soil deformation was not evident at 70 cm depth, therefore differences among treatments found in the 90-cm soil layer for k_a, D_s/D_o, *SP*, τ and d_{eff} are not considered as compaction treatment-related. Unfortunately, the deep subsoil layers exhibited quite a textural variation (Table 1).

In general, our results confirm the persistent effect of compaction on pore characteristics in the upper subsoil layer as described by Schjønning et al. (2017a) in the same experiment. Further, our study provides evidence that damage to soil pore functioning caused by mechanical stresses extends to > 50 cm depth. The long-term persistence of the compaction impacts cannot be estimated from the present results. However, we note that no mitigation can be observed two years after the conclusion of the compaction experiment. A poor resilience to

compaction of the subsoil is in line with Berisso et al. (2012). They found that only a very limited regain of pore volume – and only for the very upper subsoil – had taken place 14 years following heavy traffic.

4.3. Effects of subsoil compaction on degree of compaction

High D_b values were measured in all cases ranging from 1.58 to 1.77 Mg m^{-3} with the highest values obtained for all treatments at 30 cm depth. This supports the general observation that coarse, graded soils display high densities, as also expressed in Eq. (6) (Ehlers and Claupein, 1994; Keller and Håkansson, 2010). The Control treatment exhibited *DC* values in the range from 90 to 95% in the soil profile, whereas *DC* for compaction treatments ranged from 96 to 101, 88 to 95, 89 to 95 and 90 to 92% for the 30, 50, 70 and 90 cm depths, respectively (Fig. 2). In all instances the *DC* values obtained are higher than 87%, which is the optimal *DC* for spring barley estimated by Håkansson and Lipiec (2000). The calculated *DC* for our dataset clearly confirms the restriction for plant root growth at 30 and 50 cm depth caused by the M8 treatment, but also the existence of a preceding dense soil matrix.

Our results also confirm that traffic-induced subsoil compaction does not disappear in a short time (we measured two years after the last compaction treatment). Subsoil compaction has been found persistent for decades under Nordic conditions (e.g., Berisso et al., 2012; Schjønning et al., 2013).

4.4. Mechanistic drivers in soil compaction

Fig. 3 relates measured k_a to maximum experienced vertical stress (data from Schjønning et al. (2016)) for all depths under study. The vertical stress increased in the following order: M8 < S12 < M3 for 30 cm depth and S12 < M8 < M3 for 50, 70 and 90 cm depth. If vertical stress was the main driver for k_a, we would expect a decline in k_a with increasing vertical stress. This is observed when comparing the M3 and M8 treatments, the former always displaying higher k_a values as expected from the smaller level of vertical stress. Surprisingly, for all four depths the S12 treatment soil exhibited higher k_a values than M8 despite the soil for both treatments had experienced nearly the same level of vertical stress. Other drivers besides vertical stress may, therefore, influence traffic effects on soil pores and their functions. As the S12 treatment applied a load of ~ 12 Mg and M8 'only' ~ 8 Mg, the air permeability data as well as other soil properties quantified in this study suggest that the wheel load is not the most important cause of damage to the soil.

The total weight of the machinery used for inflicting the traffic damage each year was typically 29, 54 and 32 Mg for the M3, M8 and S12 treatments (detailed data from Schjønning et al., 2016). However, the tyres on the tractor-towed trailer had a width of 800 mm, while those of the self-propelled machine used in S12 were 1050 mm wide. In order to apply a wheel-by-wheel load across the experimental plots, M3 and M8 will necessarily be subjected to more traffic than S12. Arvidsson and Håkansson (1991) suggested the term Mgkm as an expression combining the traffic intensity and the load applied by the traffic. Mgkm is simply the product of the weight of a machine and the distance driven per unit of area. For the experimental treatments in this study, Mgkm can be calculated to approximately 191, 350 and 150 Mgkm ha^{-1} for the M3, M8 and S12 treatments, respectively. This empirical index provides an alternative quantification of the energy impact on the soil profile for the three treatments. We note that the index for S12 is less than half that of M8 and even lower than M3. The Arvidsson and Håkansson (1991) index relates better to the pattern in k_a than the vertical stress (Fig. 3).

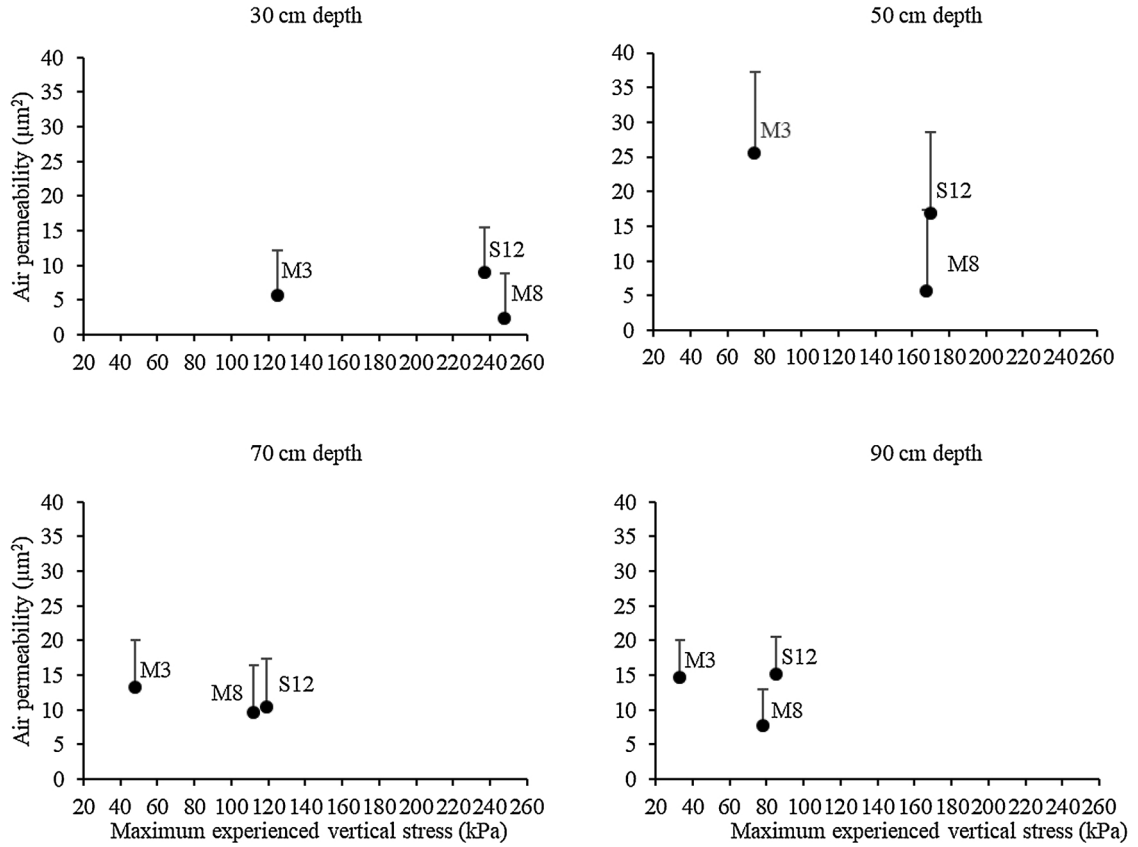

Fig. 3. Measured values of air permeability plotted against maximum experienced vertical stress (modelled data; Table C, Supplementary material in Schjønning et al., 2016). Treatment labels (M3, M8 and S12) indicate the number of wheel passes (M = multiple passes, S = single pass) and the approximate maximum wheel load in Mg.

More mechanistically, Hadas (1994) suggested that a 'hydraulic ram' effect may be triggered when very high loads are applied to soil in wet conditions. The idea is that the upper soil layers may become saturated during wheeling, hence transmitting the stresses unattenuated to deeper layers. We cannot exclude such a process, especially for the M8 treatment. The vertical stress at 30 cm depth for the M8 treatment has been quantified to more than 300 kPa when applied to another soil (Lamandé and Schjønning, 2018). When such stresses repeatedly act (consecutive wheels) on soil that is saturated to 85–90% (calculated from Schjønning et al., 2017a), the degree of saturation may become close to 100%.

The repeated wheeling in one machine pass in itself may also help explain the difference between M3 and M8 relative to S12. Several investigations have shown that soil deformation increases with the number of repeated wheel passes, although primarily for the upper soil layers (Botta et al., 2009; Zink et al., 2011; Naderi-Boldaji et al., 2018). A reduction in the number of wheel passes was pointed out as an effective means of protecting soil from soil compaction by Hamza and Anderson (2005).

Another mechanism in play may be horizontal stresses causing shear strain (Horn et al., 2003). Berisso et al. (2013) showed that significant lateral stresses acted in soil layers as deep as 50 cm during the passage of a towed implement tyre loaded with 6.1 Mg. They also quantified important effects of the resulting shear strain on soil pore functions. In the present study, this mechanism will affect a higher fraction of the soil area for M3 and M8 compared to S12 because of the narrower tyres used for the tractor-towed trailer. Further, the width of the tyres may in itself affect the lateral stresses although we are not aware of studies quantifying that hypothesis.

The draught force needed to pull the heavily loaded slurry trailer over a moist recently ploughed soil is considerable. Although traction was not quantified in this study, we hypothesize it must be much higher for M3 and M8 than for S12. The latter machine had traction on all three wheels, and no trailer had to be pulled over the soil. Only a few studies have addressed traction and its influence on soil properties. Pytka et al. (2006) found that the drawbar pull increased with wheel load for a military truck. Botta et al. (2012) found a higher motion resistance for ploughed soil than for direct-drilled soil. To our knowledge, no studies have quantified draught forces for tractor-trailer systems in real soil. However, we hypothesize that considerably higher traction forces have been active for the tractor tyres in M3 and especially the M8 treatments compared to the wheels on the self-propelled machine used in the S12 treatment. We further anticipate that horizontal stress in the driving direction related to these traction forces is responsible for shear strains reflected in the soil properties quantified in this investigation. Therefore, further studies are needed to quantify shear processes in soil compaction in our experiment.

This study was planned in order to reflect realistic traffic systems in agriculture. I.e., with only a single pass of machinery in one event of traffic as recommended by Koch et al. (2005). However, our study included repeated, experimental traffic for four consecutive years. This certainly may take place in some parts of an agricultural field such as traffic lanes for spraying and fertilizer application. However, for most of a given field, high wheel-load traffic will not necessarily take place with such a high frequency. The compaction experiment reported in this study also included a treatment (labelled M8-1) with infliction of experimental traffic only in the first year of experimentation (2010). In a previous study (Schjønning et al., 2016), we noted that the M8-1 treatment did not affect soil properties much more than M3. In contrast, a second experimental traffic pass with the ~ 8 Mg wheel load caused significant increases in soil penetration resistance. It may be speculated that this relates to increased sensitivity to compaction of the soil even a year after its first experience of high stresses. Some support for such an interpretation was given by Jakobsen and Greacen (1985), but more studies are needed to investigate this hypothesis.

5. Conclusions

Four years of repeated, annual traffic with a single-pass wheel load of ~ 12 Mg (S12) by a self-propelled tricycle-like machine for slurry application had a negligible effect on soil structure in the soil profile. In contrast, wheel loads of ~ 8 Mg in combination with four consecutive wheel passes in a tractor-trailer system markedly affected subsoil structure in terms of morph-structural characteristics, soil strength and pore system from ~ 25 cm to ~ 70 cm depth. The latter system had minor effects when wheel loads were reduced to ~ 3 Mg. The results also indicate that heavy traffic in dense soils creates a potentially restrictive subsoil structure for plant growth. Finally, our study highlights the need for future studies on the importance of repeated wheel passes and traction on soil deformation in the subsoil.

Acknowledgements

Sampling was conducted by Stig T. Rasmussen, Michael Koppelgaard and Jørgen M. Nielsen. Laboratory measurements were performed with the help of Bodil B. Christensen. This work was funded by Ministry of Environment and Food of Denmark via the COMMIT project (GUDP Grant no. 34009-16-1086) and the European Union Seventh Framework Programme (FP7/2007-2013) via the RECARE project under Grant agreement no. 603498.

Appendix A. Supplementary data

Supplementary material related to this article can be found, in the online version, at doi:https://doi.org/10.1016/j.still.2018.11.005.

References

Alakukku, L., 1996. Persistence of soil compaction due to high axle load traffic. II. Long-term effects on the properties of fine-textured and organic soils. Soil Tillage Res. 37, 223–238.
Ansorge, D., Godwin, R.J., 2007. The effect of tyres and a rubber track at high axle loads on soil compaction, part 1: single axle-studies. Biosyst. Eng. 98, 115–126.
Arvidsson, J., 2001. Subsoil compaction caused by heavy sugarbeet harvesters in southern Sweden: I. Soil physical properties and crop yield in six field experiments. Soil Tillage Res. 60, 67–78.
Arvidsson, J., Håkansson, I., 1991. A model for estimating crop yield losses caused by soil compaction. Soil Tillage Res. 20, 319–332.
Arvidsson, J., Keller, T., 2007. Soil stress as affected by wheel load and tyre inflation pressure. Soil Tillage Res. 96, 284–291.
Ball, B., Batey, T., Munkholm, L.J., Guimarães, R., Boizard, H., McKenzie, D., Peigné, J., Tormena, C., Hargreaves, P., 2015. The numeric visual evaluation of subsoil structure (SubVESS) under agricultural production. Soil Tillage Res. 148, 85–96.
Ball, B., O'sullivan, M., Hunter, R., 1988. Gas diffusion, fluid flow and derived pore continuity indices in relation to vehicle traffic and tillage. J. Soil Sci. 39, 327–339.
Ball, B.C., 1981. Modelling of soil pores as tubes using gas permeabilities, gas diffusivities and water release. J. Soil Sci. 32, 465–481.
Berisso, F.E., Schjønning, P., Keller, T., Lamandé, M., Etana, A., de Jonge, L.W., Iversen, B.V., Arvidsson, J., Forkman, J., 2012. Persistent effects of subsoil compaction on pore size distribution and gas transport in a loamy soil. Soil Tillage Res. 122, 42–51.
Berisso, F.E., Schjønning, P., Keller, T., Lamandé, M., Simojoki, A., Iversen, B.V., Alakukku, L., Forkman, J., 2013. Gas transport and subsoil pore characteristics: anisotropy and long-term effects of compaction. Geoderma 195, 184–191.
Botta, G.F., Becerra, A.T., Tourn, F.B., 2009. Effect of the number of tractor passes on soil rut depth and compaction in two tillage regimes. Soil Tillage Res. 103, 381–386.
Campbell, D.J., Dickson, J.W., Ball, B.C., Hunter, R., 1986. Controlled seedbed traffic after ploughing or direct drilling under winter barley in Scotland, 1980–1984. Soil Tillage Res. 8, 3–28.
Dexter, A.R., Czyż, E.A., Richard, G., Reszkowska, A., 2008. A user-friendly water retention function that takes account of the textural and structural pore spaces in soil. Geoderma 143, 243–253.
Eden, M., Schjønning, P., Moldrup, P., Jonge, L.W.D., 2011. Compaction and rotovation effects on soil pore characteristics of a loamy sand soil with contrasting organic matter content. Soil Use Manage. 27, 340–349.
Etana, A., Larsbo, M., Keller, T., Arvidsson, J., Schjønning, P., Forkman, J., Jarvis, N., 2013. Persistent subsoil compaction and its effects on preferential flow patterns in a loamy till soil. Geoderma 192, 430–436.
FAO, ITPS, 2015. Status of the World's Soil Resources (SWSR) –Main Report. Food and Agriculture Organization of the United Nations and Intergovernmental Technical Panel on Soils. Rome, Italy. pp. 650.
Fish, A.N., Koppi, A.J., 1994. The use of a simple field air permeameter as a rapid indicator of functional soil pore space. Geoderma 63, 255–264.

Flint, L.E., Flint, A.L., 2002. Porosity. In: Dane, J.H., Topp, G.C. (Eds.), Methods of Soil Analysis. Part 4. Physical Methods. SSSA Book Ser. 5. SSSA, Madison, WI, pp. 241–254. https://doi.org/10.2136/sssabookser5.4.c11.
Forchheimer, P., 1901. Wasserbewegung durch Boden. Zeitschrift des Vereines Deutscher Ingenieure 45, 1781–1788.
Grable, A.R., Siemer, E.G., 1968. Effects of bulk density, aggregate size, and soil water suction on oxygen diffusion, redox potentials, and elongation of corn Roots1. Soil Sci. Soc. Am. J. 32, 180–186.
Groenevelt, P., Kay, B., Grant, C., 1984. Physical assessment of a soil with respect to rooting potential. Geoderma 34, 101–114.
Hadas, A., 1994. Soil compaction caused by high axle loads—review of concepts and experimental data. Soil Tillage Res. 29, 253–276.
Hamza, M.A., Anderson, W.K., 2005. Soil compaction in cropping systems: a review of the nature, causes and possible solutions. Soil Tillage Res. 82, 121–145.
Hansen, L., 1976. Soil types at the Danish state experimental stations. Tidsskr. Planteavl 80, 742–758.
Horn, R., Fleige, H., 2009. Risk assessment of subsoil compaction for arable soils in Northwest Germany at farm scale. Soil Tillage Res. 102, 201–208.
Horn, R., Way, T., Rostek, J., 2003. Effect of repeated tractor wheeling on stress/strain properties and consequences on physical properties in structured arable soils. Soil Tillage Res. 73, 101–106.
Håkansson, I., Lipiec, J., 2000. A review of the usefulness of relative bulk density values in studies of soil structure and compaction. Soil Tillage Res. 53, 71–85.
Håkansson, I., Reeder, R.C., 1994. Subsoil compaction by vehicles with high axle load—extent, persistence and crop response. Soil Tillage Res. 29, 277–304.
Jakobsen, B.F., Greacen, E.L., 1985. Compaction of sandy forest soils by forwarder operations. Soil Tillage Res. 5, 55–70.
Keller, T., Håkansson, I., 2010. Estimation of reference bulk density from soil particle size distribution and soil organic matter content. Geoderma 154, 398–406.
Koch, H.-J., Schäfer-Landefeld, L., Stockfisch, N., Brandhuber, R., 2005. Response to the comment on “Effects of agricultural machinery with high axle load on soil properties of normally managed fields” (Authors L. Schäfer-Landefeld, R. Brandhuber, S. Fenner, H.-J. Koch, N. Stockfisch, Soil Till. Res. 75, 75–86) made by W. Ehlers, M. Goss, R. Horn. Soil and Tillage Research 80, 255-257.
Lamandé, M., Schjønning, P., 2011. Transmission of vertical stress in a real soil profile. Part II: Effect of tyre size, inflation pressure and wheel load. Soil Tillage Res. 114, 71–77.
Lamandé, M., Schjønning, P., 2018. Soil mechanical stresses in high wheel load agricultural field traffic: a case study. Soil Res. 56, 129–135.
Lipiec, J., Hatano, R., 2003. Quantification of compaction effects on soil physical properties and crop growth. Geoderma 116, 107–136.
Lipiec, J., Szustak, S., Tarkiewicz, S., 1992. Soil compaction: responses of soil physical properties and crop growth. Zeszyty Problemowe Poste˛pów Nauk Rolniczych 398, 113–117.
Naderi-Boldaji, M., Kazemzadeh, A., Hemmat, A., Rostami, S., Keller, T., 2018. Changes in soil stress during repeated wheeling: a comparison of measured and simulated values. Soil Res. 56, 204–214.
O’Sullivan, M.F., Vinten, A.J.A., 1999. Subsoil compaction in Scotland. Van den Akker, J.J.H., Arvidson, J., Horn, R. (Eds.), Experiences With the Impact and Prevention of Subsoil Compaction in the European Community. Proceedings of the First Workshop of the Concerted Action “Experiences With the Impact of Subsoil Compaction on Soil, Crop Growth and Environment and Ways to Prevent Subsoil Compaction”, 28-30 May 1998 232–240.
Obour, P.B., Schjønning, P., Peng, Y., Munkholm, L.J., 2016. Subsoil compaction assessed by visual evaluation and laboratory methods. Soil Tillage Res.
Pytka, J., Dąbrowski, J., Zając, M., Tarkowski, P., 2006. Effects of reduced inflation pressure and vehicle loading on off-road traction and soil stress and deformation state. J. Terramechanics 43, 469–485.
Riggert, R., Fleige, F., Kietz, B., Gaertig, T., Horn, R., 2016. Stress distribution under forestry machinery and consequences for soil stability. Soil Sci. Soc. Am. J. 80, 38–47.
Rosin, P., Rammler, E., 1933. The laws governing the fineness of powdered coal. Fuel 29–36 The laws governing the fineness of powdered coal.
Rüegg, K., 2000. Development, Test and Use of an Air-pycnometer to Measure Air-filled Porosity on Undisturbed Soil Samples. M.S. Thesis. Aalborg Univ., Aalborg, Denmark.
Schäfer-Landefeld, L., Brandhuber, R., Fenner, S., Koch, H.-J., Stockfisch, N., 2004. Effects of agricultural machinery with high axle load on soil properties of normally managed fields. Soil Tillage Res. 75, 75–86.
Schäffer, B., Mueller, T.L., Stauber, M., Müller, R., Keller, M., Schulin, R., 2008. Soil and macro-pores under uniaxial compression. II. Morphometric analysis of macro-pore stability in undisturbed and repacked soil. Geoderma 146, 175–182.
Schjønning, P., 1992. Size distribution of dispersed and aggregated particles and of soil pores in 12 danish soils. Acta Agric. Scand. Sect. B — Soil Plant Sci. 42, 26–33.
Schjønning, P., Koppelgaard, M., 2017. The Forchheimer Approach for Soil Air Permeability Measurement. Soil Sci. Soc. Am. J.
Schjønning, P., Lamandé, M., Berisso, F.E., Simojoki, A., Alakukku, L., Andreasen, R.R., 2013. Gas diffusion, non-Darcy air permeability, and computed tomography images of a clay subsoil affected by compaction. Soil Sci. Soc. Am. J. 77, 1977–1990.
Schjønning, P., Lamandé, M., Crétin, V., Nielsen, J.A., 2017a. Upper subsoil pore characteristics and functions as affected by field traffic and freeze–thaw and dry–wet treatments. Soil Res. 55, 234–244.
Schjønning, P., Lamandé, M., Keller, T., Pedersen, J., Stettler, M., 2012. Rules of thumb for minimizing subsoil compaction. Soil Use Manage. 28, 378–393.
Schjønning, P., Lamandé, M., Munkholm, L.J., Lyngvig, H.S., Nielsen, J.A., 2016. Soil precompression stress, penetration resistance and crop yields in relation to differently-trafficked, temperate-region sandy loam soils. Soil Tillage Res. 163, 298–308.
Schjønning, P., McBride, R., Keller, T., Obour, P., 2017b. Predicting soil particle density from clay and soil organic matter contents. Geoderma 286, 83–87.
Schjønning, P., Thomsen, I.K., 2013. Shallow tillage effects on soil properties for temperate-region hard-setting soils. Soil Tillage Res. 132, 12–20.
Schjønning, P., Thomsen, I.K., Moldrup, P., Christensen, B.T., 2003. Linking soil microbial activity to water- and air-phase contents and diffusivities. Soil Sci. Soc. Am. J. 67, 156–165.
Schjønning, P., van den Akker, J.J., Keller, T., Greve, M.H., Lamandé, M., Simojoki, A., Stettler, M., Arvidsson, J., Breuning-Madsen, H., 2015. Chapter five-driver-pressure-state-impact-response (DPSIR) analysis and risk assessment for soil compaction—a european perspective. Adv. Agron. 133, 183–237.
Söhne, W., 1958. Fundamentals of pressure distribution and soil compaction under tractor tyres. Agric. Eng. 39 (276-281), 290.
Stepniewski, W., 1980. Oxygen-diffusion and strength as related to soil compaction. I. ODR. Polish J. Soil Sci. 13, 3–13.
Stepniewski, W., 1981. Oxygen diffusion and strength as related to soil compaction. 1. ODR (oxygen diffusion rate). Polish J. Soil Sci.
Vermeulen, G.D., Verwijs, B.R., van den Akker, J.J.H., 2013. Comparison of Loads on Soils During Agricultural Field Work in 1980 and 2010 (In Dutch With English Summary). Plant Research International, Rapport 501, Wageningen.
Voorhees, W.B., Nelson, W.W., Randall, G.W., 1986. Extent and persistence of subsoil compaction caused by heavy axle loads. Soil Sci. Soc. Am. J. 50, 428–433.
Zink, A., Fleige, H., Horn, R., 2010. Load risks of subsoil compaction and depths of stress propagation in arable Luvisols. Soil Sci. Soc. Am. J. 74, 1733–1742.
Zink, A., Fleige, H., Horn, R., 2011. Verification of harmful subsoil compaction in loess soils. Soil Tillage Res. 114, 127–134.